Received: 17 January 2022 | Revised: 7 April 2022 | Accepted: 28 April 2022

DOI: 10.1002/cyto.a.24567

ORIGINAL ARTICLE

ISAC CYTOMETRY Journal of Quantitative Cell Science PART A

Identification of fetal liver stroma in spectral cytometry using the parameter autofluorescence

Márcia Mesquita Peixoto[1,2,3,4,5,6] | Francisca Soares-da-Silva[1,2,3] | Sandrine Schmutz[7] | Marie-Pierre Mailhe[1,2,3] | Sophie Novault[7] | Ana Cumano[1,2,3] | Cedric Ait-Mansour[8]

[1]Immunology Department, Unit Lymphocytes and Immunity, Institut Pasteur, Paris, France

[2]INSERM U1223, Paris, France

[3]Université de Paris, Sorbonne Paris Cité, Paris, France

[4]Instituto de Investigação e Inovação em Saúde, Universidade do Porto, Porto, Portugal

[5]Instituto Nacional de Engenharia Biomédica, Universidade do Porto, Porto, Portugal

[6]Instituto de Ciências Biomédicas Abel Salazar, Universidade do Porto, Porto, Portugal

[7]Flow cytometry core facility, CRT2, Institut Pasteur, Paris, France

[8]Sony Europe B.V, Weybridge, United Kingdom

Correspondence
Ana Cumano, Immunology Department, Institut Pasteur 25 Rue du Dr. Roux 75724 Paris, CEDEX 15, France.
Email: ana.cumano@pasteur.fr

Funding information
This work was supported by grants from Institut Pasteur, INSERM, ANR and FCT/MCTES.

Abstract

The fetal liver (FL) is the main hematopoietic organ during embryonic development. The FL is also the unique anatomical site where hematopoietic stem cells expand before colonizing the bone marrow, where they ensure life-long blood cell production and become mostly resting. The identification of the different cell types that comprise the hematopoietic stroma in the FL is essential to understand the signals required for the expansion and differentiation of the hematopoietic stem cells. We used a panel of monoclonal antibodies to identify FL stromal cells in a 5-laser equipped spectral flow cytometry (FCM) analyzer. The "Autofluorescence Finder" of SONY ID7000 software identified two distinct autofluorescence emission spectra. Using autofluorescence as a fluorescence parameter we could assign the two autofluorescent signals to three distinct cell types and identified surface markers that characterize these populations. We found that one autofluorescent population corresponds to hepatoblast-like cells and cholangiocytes whereas the other expresses mesenchymal transcripts and was identified as stellate cells. Importantly, after birth, autofluorescence becomes the unique identifying property of hepatoblast-like cells because mature cholangiocytes are no longer autofluorescent. These results show that autofluorescence used as a parameter in spectral FCM is a useful tool to identify new cell subsets that are difficult to analyze in conventional FCM.

KEYWORDS
autofluorescence, fetal liver, hepatoblast-like cells/hepatocytes, spectral flow cytometry

1 | INTRODUCTION

Flow cytometry (FCM) has rapidly evolved over the past few decades [1]. The development of more advanced technologies including mass cytometry [2], imaging FCM [3], genomic FCM [4] and spectral FCM [5], has expanded our ability to study immune responses, by characterizing more cellular parameters simultaneously in single cells with higher resolution than ever before. FCM characterizes physical and fluorescent properties of cells in suspension by using fluorochrome-conjugated antibodies to measure proteins expressed by distinct immune cell subpopulations [6].

Spectral FCM was first proposed by J. Paul Robinson at Purdue University in 2004 [7]. The first commercial instrument (Sony SP6800) was launched by Sony Biotechnology in 2012, using prisms along with PMT detectors to collect and amplify light beyond the capability of

Marcia Mesquita Peixoto, Francisca Soares-da-Silva contributed equally. Sophie Novault, Ana Cumano, and Cedric Ait-Mansour are Co-senior authors.

This is an open access article under the terms of the Creative Commons Attribution-NonCommercial License, which permits use, distribution and reproduction in any medium, provided the original work is properly cited and is not used for commercial purposes.
© 2022 The Authors. *Cytometry Part A* published by Wiley Periodicals LLC on behalf of International Society for Advancement of Cytometry.

conventional flow cytometers [8]. The Sony SP6800 is equipped with three lasers 405/488/638 nm and two pinholes such that two excitation lasers can be used in a given experiment. Using the 405/488 nm excitation lasers we assembled a 19-fluorescent probe panel to analyze immune cells in the mouse adult spleen [9, 10]. Moreover, analysis of antibody-stained preparations of embryonic, neonatal, and adult heart, which is a highly auto-fluorescent tissue, allowed the robust identification of new surface markers of different cardiac populations [11]. In addition, intra-epithelial lymphocytes were efficiently analyzed in mouse intestinal epithelium cell preparations because the autofluorescence management allowed eliminating from the analysis the autofluorescent epithelial cells [9]. Recently, the Sony ID7000 became available with different laser configurations that can be remodeled. The ID7000 Software analysis is based on the previously described Weighted Least Squares Method algorithm [8] that allows the easy detection of auto-fluorescence (AF) that can be incorporated in the panel as independent fluorescent parameters.

The fetal liver (FL) is a highly auto-fluorescent tissue where hepatic and hematopoietic cells differentiate alongside and where hepatic and mesenchymal cells play, yet ill-defined, roles in hematopoietic differentiation [12] and in the establishment of the hematopoietic stem cell compartment [13]. In addition, although surface markers for different populations have been identified, a global analysis of the FL stroma using epithelial and mesenchymal markers has not been undertaken.

Here we sought to analyze the nonhematopoietic stromal compartment in mouse FL using a 14-fluorochrome antibody panel and distinct AF parameters that were unique in the identification of cell populations. We found two major AF signals at embryonic day (E)18.5 of mouse gestation. One AF signal has different emission spectra in the 355 nm laser and in the 405 nm laser. It defines stellate cells that accumulate autofluorescent vitamin A in cytoplasmic granules [14]. The second AF signal is visible in the 355 nm laser, in the 405 nm and also with a lower intensity and different emission spectra in the 488 and 561 nm lasers and marks hepatoblasts/hepatocytes and cholangiocytes. Importantly, AF is an invaluable tool to distinguish cells with the characteristics of E14.5 hepatoblasts, after birth, hereafter designated as hepatoblast-like cells. In addition, defining the true fluorescence associated with each autofluorescent population helped design a sorting strategy to be used in conventional FCM. These results indicate that AF treated as a fluorescence parameter in spectral FCM is essential to the characterization of cell subsets in solid tissues.

2 | MATERIALS AND METHODS

The experiment was designed to identify populations of stromal cells in the mouse FL at different stages of gestation.

2.1 | Cell suspension

E14.5, E18.5 FLs, P3 and P9 livers were dissected under a binocular magnifying lens. Cells were recovered in Hanks' balanced-salt solution (HBSS) supplemented with 1% fetal calf serum (FCS) (Gibco) or RPMI medium (Gibco) supplemented with 10% FCS (P3 and P9) and treated with 0.05 mg/ml Liberase TH (Roche) and 0.2 mg/ml DNAse (Sigma) for 6–8 min at 37°C. Cells were resuspended by gentle pipetting. Before staining, cell suspensions were filtered with a 100 µm cell strainer (BD). All experiments using E14.5 and E18.5 embryos were done by pooling FL cells from the same litter in each experiment, in three or more biological replicates. In an independent experiment, FL cells were analyzed after mechanical dissociation (in two biological replicates; *data not shown*).

2.2 | Flow sample and specimen description

All antibodies were titrated to give the highest signal-to-noise ratio. The antibody panel has been optimized in a conventional flow cytometer (LSR Fortessa with five lasers (BD Biosciences) and then used in the ID7000 (Sony) to study the autofluorescence. Liver cells were depleted of $Ter119^+$ $CD45^+$ $CD71^+$ $CD117^+$ cells by magnetic cell separation using LS MACS Columns (Miltenyi Biotec). Cell suspensions were stained in two steps. First, cell suspensions of FL were incubated with the biotinylated antibodies for 15–20 min at 4°C. Cells were washed to eliminate excess of antibody, incubated for 15 min with anti-biotin beads (Miltenyi Biotec) and applied to a LS MACS

TABLE 1 List of the antibodies used in this study and their specificity

Marker	Conjugation	
SAV	PE-Cy5	CD45, TER119, CD71, CD117 (all hematopoietic cells) biotin
Dead	PI	—
CD324	PE-Cy7	(Epithelial-Cadherin) hepatoblasts, hepatocytes and cholangiocytes
CD31	PerCP-Cy5.5	(Platelet and endothelial cell adhesion molecule) endothelial cells
CD166	FITC	(Activated Leukocyte Cell Adhesion Molecule) hepatoblasts and stellate cells
CD140a	APC	(Platelet derived growth factor receptor a) stellate cells and pericytes
Gp38	APC-Cy7	(Podoplanin) mesenchymal cells, lymphatic endothelial cells
NG2	PE	(Chondroitin sulphate proteoglycan 4) pericytes
Sca-1	BV711	(Stem Cell antigen 1) endothelial cells
CD146	BV510	(Melanoma cell adhesion molecule) endothelial cells and mesenchymal cells
CD51	BV421	(Integrin alpha V) mesenchymal cells
CD326	BV605	(Epithelial cell adhesion molecule) cholangiocytes (bile duct cells)
CD54	BUV395	(Intercellular Adhesion Molecule 1) hepatoblasts and endothelial cells
Thy1.2	AF700	(Cluster of differentiation 90) mesenchymal cells

Column (Miltenyi Biotec). The 5% of the cells were not passed through the MACS column and were used as depletion control. The 5% of the eluted cells were used as unstained control and the remaining were incubated for 20–30 min at 4°C in the dark with directly labeled antibodies (and streptavidin (SAV) listed in Table 1/Supplemental Table 1. PI was added to depleted stained and to the depletion control samples.

2.3 | Instrument details

Stained cells were analyzed in the Sony ID7000 spectral cytometer. The LE-ID7000E used in this study has five lasers 355/405/488/561/637 nm (Supplemental Figure 1), PMT gains/voltages can be independently adjusted for each laser, and there are seven pinholes allowing for additional lasers to be installed. The schematic optical configuration is shown in Supplemental Figure 1, framed by a black box. The detection capacity of the ID7000 spans from 360 nm to 820 nm in the 5-laser configuration. The signals are captured with 32-, 26-, and 19-channel PMT arrays and individual PMT, as shown.

Before the analysis, the Sony ID7000 was calibrated using the align-check and the performance 8-peak beads, following the guidelines of the instrument provider. A minimum of 100,000 events were acquired for cell-stained samples and a minimum of 20,000 events for unstained samples. In every experiment single-stained samples in

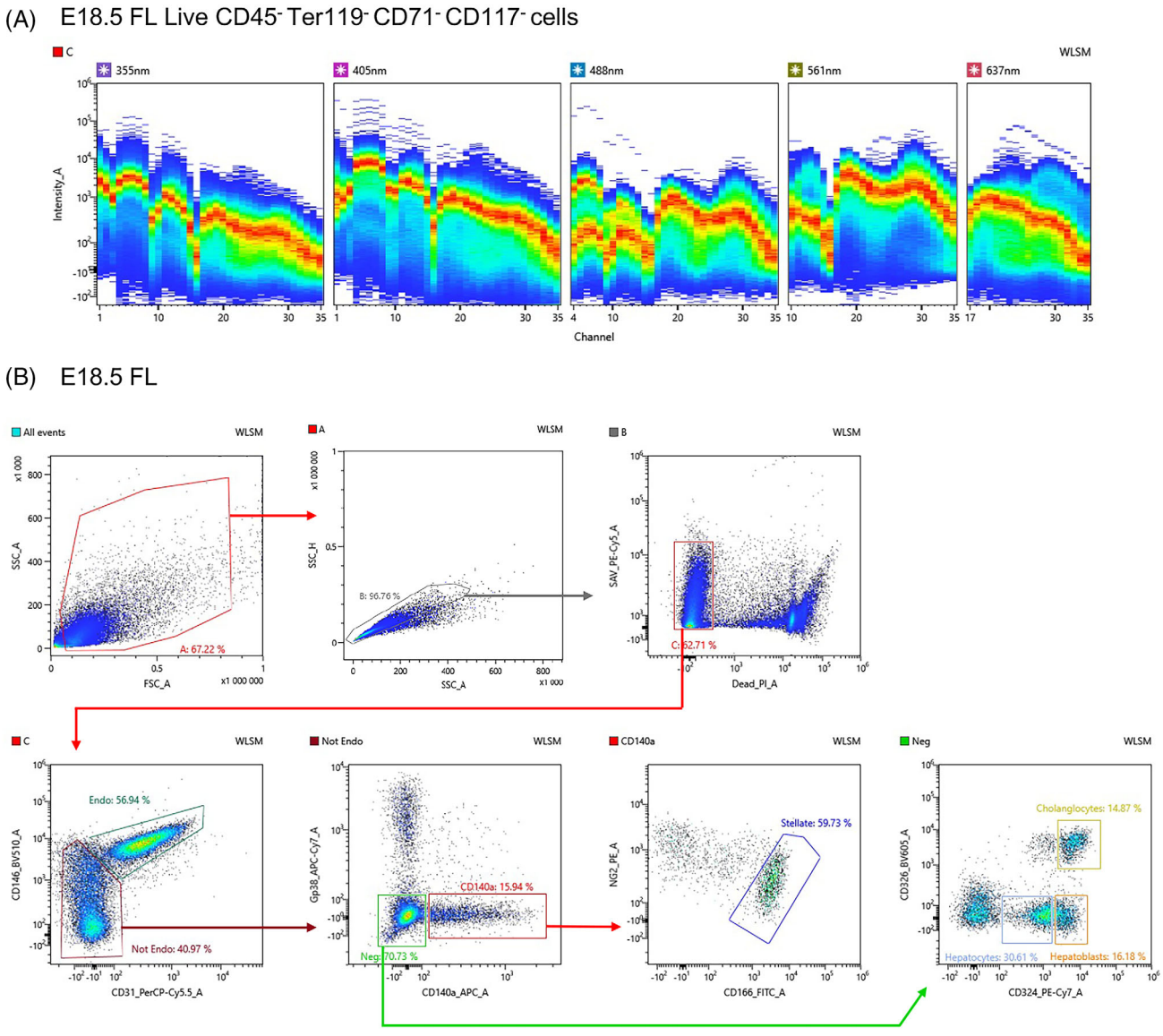

FIGURE 1 Gating strategy to identify stellate cells, hepatoblasts-like cells, hepatocytes and cholangiocytes. E18.5 mouse fetal liver cell suspensions were stained with biotin labeled antibodies recognizing CD45, TER119, CD71, CD117. Negative cells were magnetically sorted and labeled with the antibodies in Table 1. (A) The spectra of emission of fetal liver cells after depletion (marked with streptavidin in a dump channel) and gated out of PI labeled cells. (B) After unmixing, cells were manually gated to define endothelial, hepatic and stellate cells. The analysis started with a FSC_A/SSC_A gate, doublet exclusion and PI positive/SAV positive cell exclusion. The gate for SAV exclusion was set by the depletion control sample (not depleted). CD324 was defined as a marker of epithelial cells, cholangiocytes $CD324^{high}CD326^{+}$; hepatocytes $CD324^{low}CD326^{-}$; hepatoblasts-like cells $CD324^{high}CD326^{-}$. Stellate cells are defined by as $PDGFRa^{+}$ $CD166^{+}$. [Color figure can be viewed at wileyonlinelibrary.com]

Ultracomp eBeads (Thermo Fisher), for each individual fluorochrome, were provided and a minimum of 2000 events were collected. Total FL cells stained with propidium iodide (PI) were used as the control for dead cell exclusion. Unstained cells after depletion were always included. Stained cells with the full panel, before depletion of hematopoietic cells, were analyzed as a control for lineage staining.

3 | DATA ANALYSIS DETAILS

3.1 | Autofluorescence analysis

The unstained samples, after depletion of hematopoietic cells, were analyzed using the autofluorescence finder function as shown in Figure 2. This is a nonautomatic visualization tool where scanning across the emission wavelengths on each laser detects the best display of autofluorescence. The scanning is done by moving the cursor (bar under top plots in Figure 2) and the signal in the different combined detectors can be adjusted to find the best separation between the different autofluorescence signals. The autofluorescence signals are then manually gated and checked for their emission spectra (see Figure 2, lower panels). Distinct autofluorescence signals will separate in one of the laser combinations and will have distinct emission spectra. Once identified the autofluorescence signals are incorporated in the unmixing matrix.

Acquired full spectrum are analyzed with algorithms based on the WLSM as described previously [8]. The accuracy of the unmixing is ensured by the analysis of the single stained samples. Further manual adjustments (usually not required) can be done. Acquisitions were done with similar settings of the laser PMT.

Cells were sorted with a BD FACSAria III (BD Biosciences) according to the guidelines for the use of FCM and cell sorting [6]. The FACSAria III was calibrated with CST beads following the manufacturer's protocols. Data were analyzed with the ID7000 (Sony, Inc) or FlowJo (v.10.7.3, BD Biosciences) software.

3.2 | Gene expression by RT-PCR

Cells were sorted directly into lysis buffer and mRNA was extracted with a RNeasy Micro Kit (Qiagen). After extraction mRNA was reverse-transcribed into cDNA with PrimeScript RT Reagent Kit (Takara Bio), followed by quantitative PCR with Power SYBR Green PCR Master Mix (Applied Biosystems). Primers used were as follows: Actb FW: GCTTCTTTGCAGCTCCTTCGT; Actb RV: ATCGTCATCCATGGCGAACT; Afp FW: CTTCCCTCATCCTCCTGCTAC; Afp RV: ACAAACTGGGTAAAGGTGATGG; Alb FW: TGCTTTTTCCAGGGGTGTGTT; Alb RV: TTACTTCCTGCACTAATTTGGCA; Des FW: GTGGATGCAGCCACTCTAGC; Des RV: GTGGATGCAGCCACTCTAGC; Onecut1 FW: GCCCTGGAGCAAACTCAAGT; Onecut1 RV: TTGGACGGACGCTTATTTTCC; Pdgfrb FW: TTCCAGGAGTGATACCAGCTT; Pdgfrb RV: AGGGGGCGTGATGACTAGG; Sox9 FW: CTCCTCCACGAAGGGTCTCT; Sox 9 RV: AGGAAGCTGGCAGACCAGTA. qPCR reactions were performed on a Quantstudio3 thermocycler (Applied Biosystems), gene expression was normalized to that of β-actin and relative expression was calculated using the $2^{-\Delta Ct}$ method.

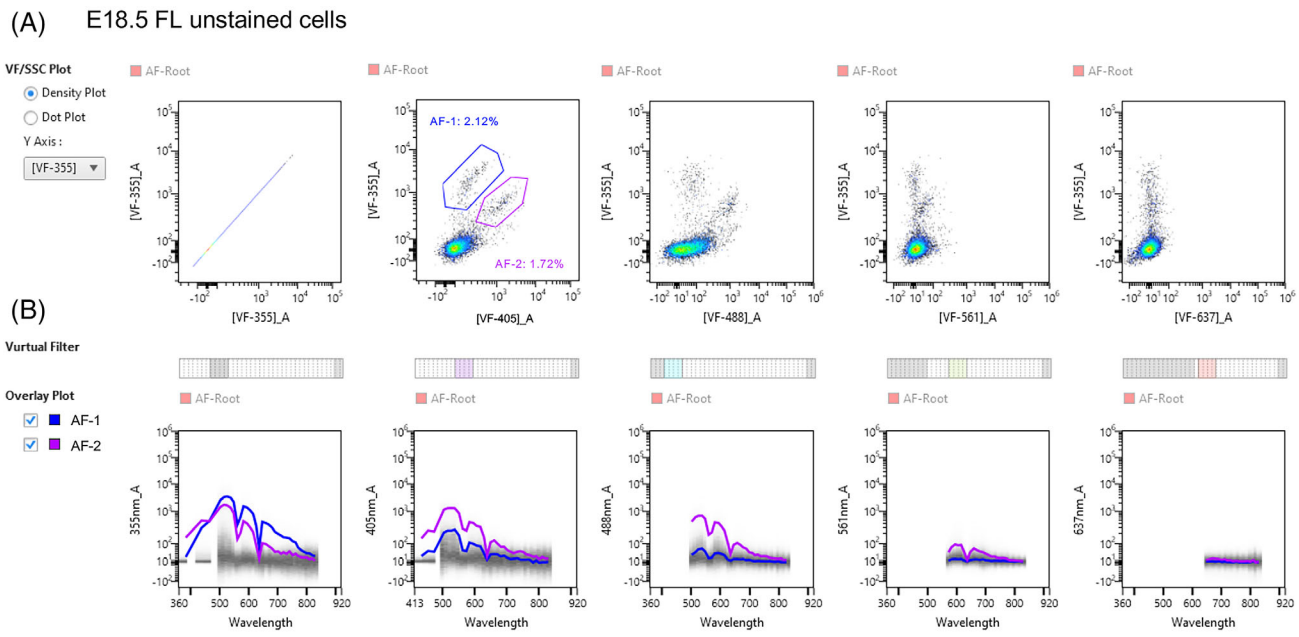

FIGURE 2 Autofluorescence finder. The analytical tool autofluorescence applied to unstained cells before unmixing. (A) Autofluorescence is defined manually in cells that show fluorescence in the different lasers, as defined in Materials and Methods. (B) The spectra of emission of the two defined autofluorescent (AF) signals in the different lasers. [Color figure can be viewed at wileyonlinelibrary.com]

3.3 | Statistical analysis

All results are shown as mean ± standard deviation (SD). Statistical significance was determined using one-way ANOVA followed by Tukey's multiple comparison test where a p value <0.05 was considered significant and a p value >0.05 was considered not significant.

4 | RESULTS

4.1 | A strategy to characterize nonhematopoietic cell populations in FL

To characterize nonhematopoietic (hereafter referred to as stromal) populations in the FL we assembled a panel of 14 fluorescent dyes (Table 1) that included propidium iodide (PI-dead cell exclusion) and 13 fluorescence conjugated antibodies that mark cells belonging to the hepatic, endothelial and mesenchymal lineages (liver fibroblasts, also called stellate cells - see Table 1). The analysis was done in FL cell suspensions depleted of hematopoietic cells in a dump channel that includes the erythroid marker TER119, the pan-hematopoietic marker CD45, and CD71 and CD117 that together mark embryonic erythroid progenitors [15]. Cells were depleted of hematopoietic cells, that represent more than 80% of total FL cells, by magnetic sorting. We analyzed liver cells isolated from embryonic days (E) 14.5 and E18.5 (1 day prior to birth), and from days 3 and 9 postbirth (P3 and P9). Figure 1A shows the spectra of emission of E18.5 cells after the elimination of hematopoietic and dead cells. Figure 1B shows the gating strategy used to identify known cell subsets with CD31 and CD146 defining endothelial cells, and, in nonendothelial cells, CD140a (PDGFRa), Gp38 (podoplanin), and CD166 (ALCAM) define stellate cells as CD140a^{+} Gp38^{-}CD116^{+} [13]. In the Gp38^{-}CD140a^{-} subset, CD326 and CD324 (E-Cadherin) define cholangiocytes (CD324^{+}CD326^{+}) [16] and hepatic cells (CD324$^{high/low}$ CD326^{-}) [17] . This analysis shows that at E18.5 all major FL populations are detected, and hepatocytes are difficult to discriminate from the decreasing numbers of hepatoblasts that are undergoing differentiation.

4.2 | Two different autofluorescence patterns identified by the autofluorescence finder

AF is a property of many tissues defined as signal emission by cells excited at particular wavelengths, in the absence of specific fluorescence. AF can mask or distort true fluorescence and is usually subtracted to facilitate the fluorescence detection. The ID7000 spectral cytometer is equipped with an analytical software that provides a tool to identify independent AF signals called AF finder (Figure 2, see Materials and Methods). In unstained cells this tool allowed the detection of two AF signals (Figure 2A). AF-1 shows an emission spectra with 3 emission peaks detected in the 355 and 405 lasers(around 510nm, 590nm and 655nm) and 2 smaller emission peaks in the 488 laser (around510nm and 590nm). AF-2 shows a similar emission spectra as AF-1 with the addition of anemission peak at 655nm in the 488 laser and 2 emission peaks in the 561 laser (around600nm and 655nm). The differences in the spectra of emission found in most laser channels suggested that these two AF signals correspond to two independent cell types. Efficient single cell suspension that minimizes cell death requires an enzymatic digestion of the FL. To test whether the two autofluorescence signals were impacted by the enzymatic digestion we analyzed E14.5 FL after mechanic dissociation. The autofluorescent signals were detected after mechanic dissociation (*data not shown*) indicating that they are an intrinsic property of the two subsets. The frequencies and numbers of cells exhibiting AF-1 and AF-2 were, however, strongly reduced consistent with our previous observation that mechanical dissociation is not suited for FL viable cell recovery.

After unmixing, we used AF-1 and AF-2 as independent parameters to define two different populations and proceeded to identify their identity (Figure 3A–D). Figure 3 shows two independent gating strategies, one that analyzes cells within AF-1 (Figure 3B) compared to the conventional strategy previously shown in Figure 1 (Figure 3A). AF-1 cells correspond to a majority of CD31^{-} (85%), CD140a^{+} (85%) cells and CD116^{+} (95%) cells (Figure 3B) that define, with a high degree of enrichment, stellate cells.

CD324^{+} hepatocytes and CD324^{+}CD326^{+} cholangiocytes (bile duct cells) are known to derive during embryonic development from bipotent progenitors called hepatoblasts [18]. AF-2 gated cells (Figure 3C) comprise a majority (83%) of CD31^{-} nonendothelial cells, 94% of CD140a^{-} gp38^{-} and > 90% of CD324^{high}. We designated this population hepatoblasts-like cells because they closely resemble cells with similar phenotype and autofluorescent properties in E14.4 FL, before cholangiocyte differentiation (Supplemental Figure 2), known to be bipotent progenitors [16]. Within AF-2 in E18.5 FL we also found CD324^{+} CD326^{+} cholangiocytes [19]. Interestingly, the analysis done in AF-2 did not detect the subset that expresses low levels of CD324 that we classify as hepatocytes [17] (Figure 3C). AF-2 is, therefore, an important parameter to distinguish hepatoblasts-like cells from hepatocytes, at this stage of development. When auto-fluorescent cells were gated out, stellate cells are virtually absent from the plots (Figure 3D) whereas a subset of hepatoblasts-like cells and cholangiocytes are still detected (30% and 50%, respectively) indicating that AF-2 distinguishes two different cell subsets (AF-2^{+} and AF-2^{-} cells) in each of these populations. The cells designated as nonAF correspond to cells with low AF-1 and AF-2 and comprise all other cell populations in the FL that exhibit background levels of AF.

4.3 | Properties and identity of FL stromal cells

To further characterize the AF of FL cells and determine whether this is a cell-intrinsic property or if it is lost upon manipulation we sorted hepatic cells, hepatoblast-like cells and stellate cells from E18.5 FL

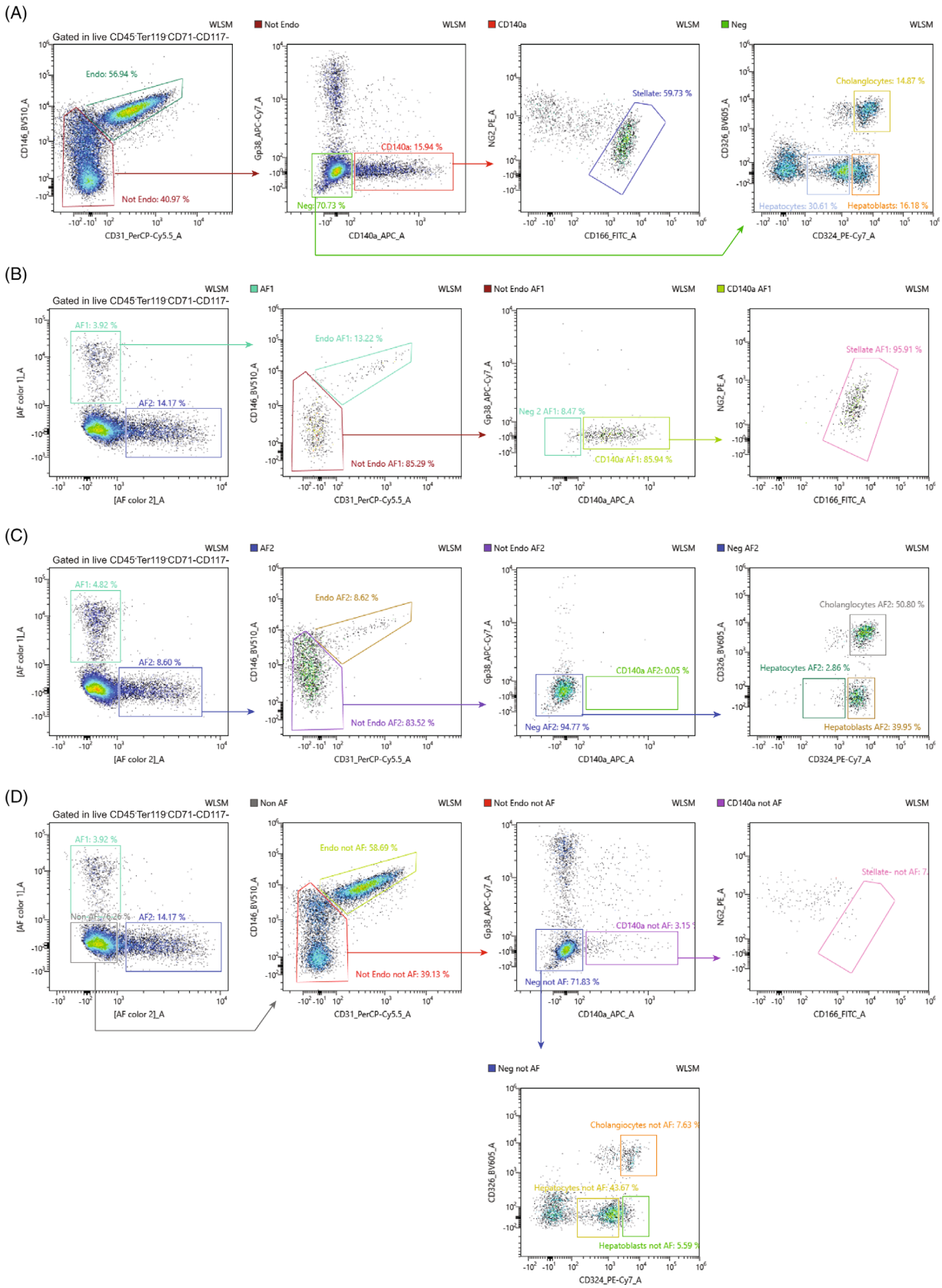

FIGURE 3 Two distinct autofluorescent signals: AF-1 defines stellate cells and AF-2 defines a subset of hepatic cells and cholangiocytes. After unmixing the two AF signals can be used as two additional fluorescent parameters. (A) E18.5 FL live CD45$^-$TER119$^-$CD71$^-$CD117$^-$ cells were analyzed as in Figure 1B. (B) Analysis of E18.5 FL live CD45$^-$TER119$^-$CD71$^-$CD117$^-$AF1$^+$ cells using the same strategy as in Figure 1B. (C) Analysis of E18.5 FL live CD45$^-$TER119$^-$CD71$^-$CD117$^-$AF2$^+$ cells using the same strategy as in Figure 1B. (D) Analysis of E18.5 FL live CD45$^-$TER119$^-$CD71$^-$CD117$^-$AF1$^-$AF2$^-$ cells using the same strategy as in Figure 1B. [Color figure can be viewed at wileyonlinelibrary.com]

using a simplified panel in a conventional flow cytometer (Figure 4A, presort). All populations before and after cell sorting were analyzed in spectral FCM (Figure 4B, sorted populations). Stellate cells (lower plots) show persistent levels of AF whereas hepatocytes (upper plots) remained negative for this parameter. As previously observed, hepatoblast-like cells sorted as CD324^{high} cells yield a mixed population of AF-2^{+} and AF-2^{-} cell (middle plots). These results indicated that AF in FL populations is a cell-specific property.

In order to unambiguously ascertain the lineage affiliation of these three cell subsets we subjected the cells sorted to quantitative RT-PCR. We show that cells classified as cholangiocytes by FCM express the cholangiocytic markers *Sox9* and *Onecut 1* (*Hnf6*) [16], the hepatoblasts-like cells express *Onecut 1* [18], *Alb* and *Afp* whereas stellate cells express *Desmin* and *Pdgfrb* (Figure 4C) [20]. This transcriptional profile is specific for the three subsets thus confirming the lineage affiliation inferred by the surface marker expression.

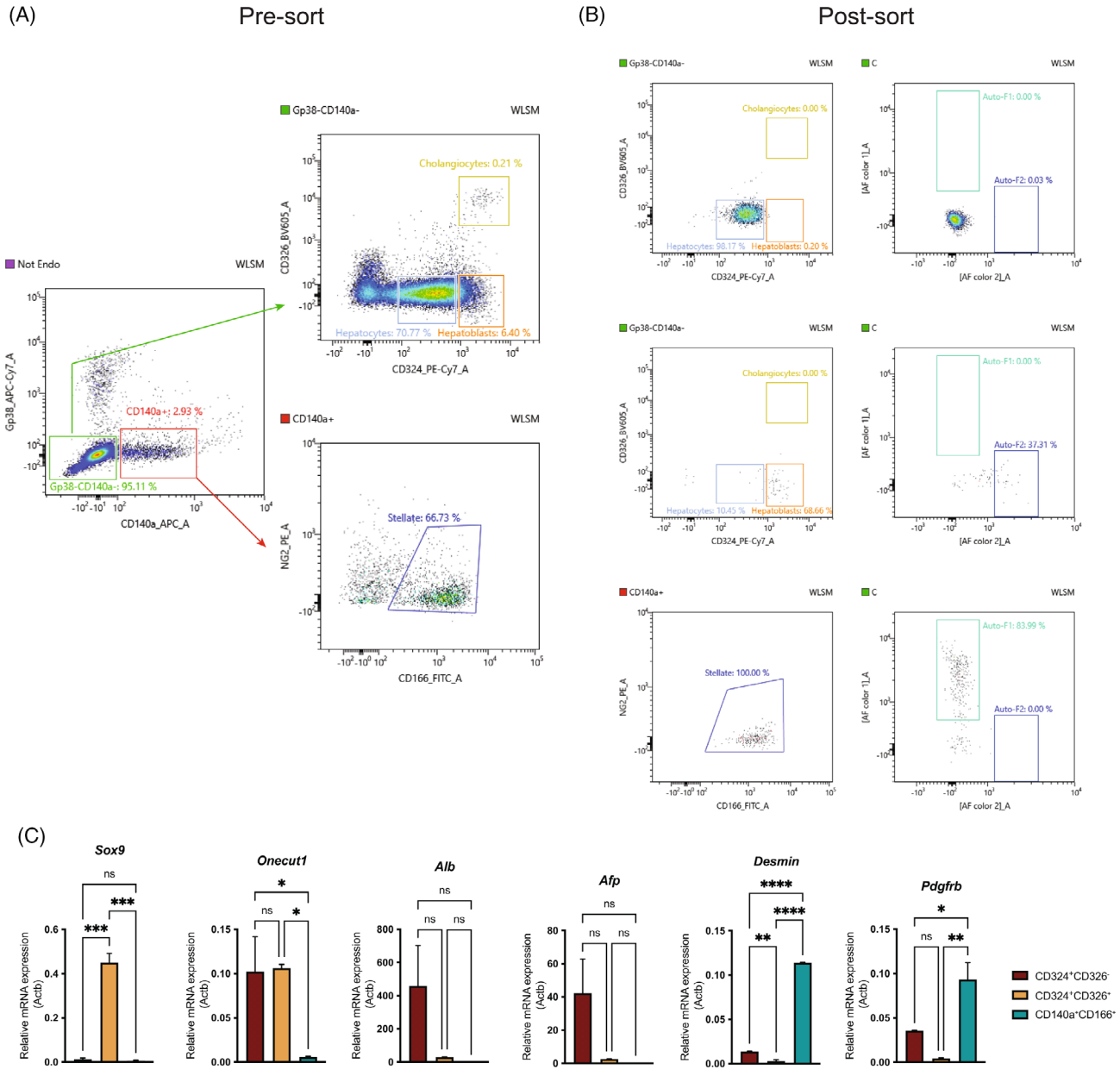

FIGURE 4 Autofluorescence is a cell intrinsic property. (A) Fetal liver cells negative for the dump channel and for PI expressing cells were sorted after being stained with a simplified antibody panel including Gp38, CD140a, NG2, CD166, CD324 and CD326. Hepatocytes, hepatoblast-like cells and stellate cells were sorted according to the strategy shown (presort). Sorted cells were reanalyzed in the ID7000 spectral analyzer (sorted populations). Left plots show purity control, right plots show AF of sorted cells. (B) Sorted cholangiocytes, hepatoblast-like cells and stellate cells as in A were subjected quantitative RT-PCR in triplicate samples of two independent experiments for *Sox9*, *Onecut1*, *Alb*, *Afp*, *Desmin* and *Pdgfrb*, and normalized to the expression of β-actin used as house-keeping gene. Data are represented as mean +/− SD. *$p < 0.05$, **$p < 0.01$, ***$p < 0.001$, ****$p < 0.0001$. [Color figure can be viewed at wileyonlinelibrary.com]

4.4 | Autofluorescence defines hepatoblast-like cells after birth

Hepatoblast-like cells decrease in numbers as development progresses, so we used AF-2 to detect these cells, after birth. However, hepatocytes that are the dominant liver population after birth are fragile epithelial cells, highly sensitive to manipulation ex vivo and to the disruption of the tight junctions, required for single-cell suspensions. Consequently, we detected decreasing numbers of hepatocytes with age. At P3 and P9 the levels of AF were very similar in spectrum and intensity to those seen at E18.5. At P3 and P9 AF-2 represents a majority of hepatoblast-like cells with high expression of CD324, and by high AF-2 (Figure 5A). Interestingly, at these stages, most cholangiocytes lost expression of AF-2. This result is reinforced at P9 (Figure 5B) where gating in AF-2 yields 93% of hepatoblast-like cells. These results further indicate that AF-2 is essential for the identification of hepatoblast-like cells, after birth.

5 | DISCUSSION

In this report we used a spectral flow cytometer equipped with five lasers to analyze a highly autofluorescent tissue, the FL, in single-cell suspensions. The software analysis of the Sony ID7000 is equipped with an analytical tool for easy detection of different autofluorescent signals. The unmixing algorithm subtracts the AF to find true fluorescent signals but importantly, by using the AF signals as independent parameters, it increased the panel of 14-fluorescent dyes into a 16-fluorescence panel.

The "Autofluorescence finder" tool identified independent AF signals that differed in shape and intensity in the different laser

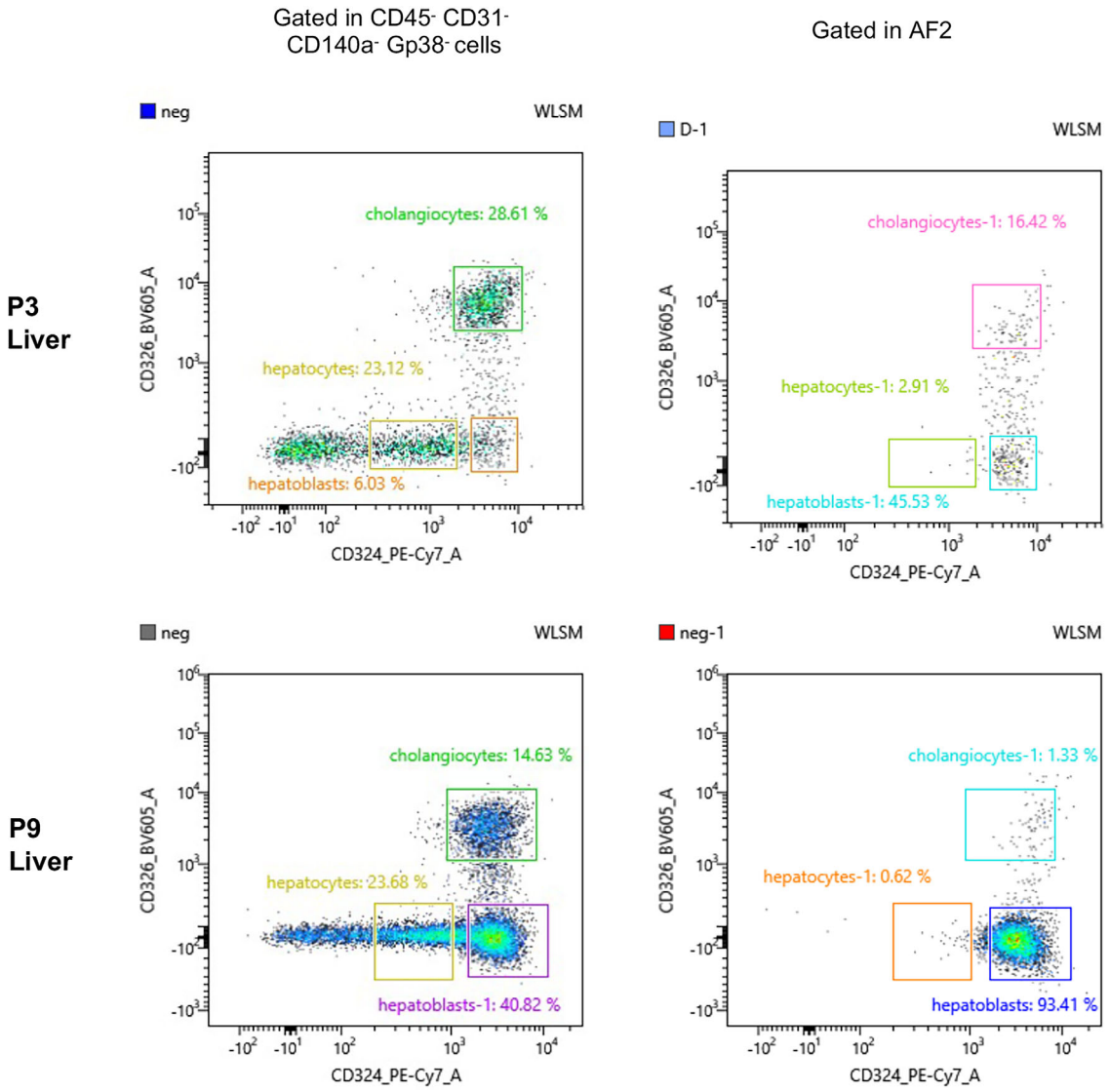

FIGURE 5 AF2 defines hepatoblast-like cells after birth. Analysis of live CD45^{-}TER119^{-}CD71^{-}CD117^{-} P3 and P9 liver cells in a plot of CD324/CD326 after the conventional gating strategy defined in Figure 1 (left plots) or on the cells gated for AF2 expression (right plots). [Color figure can be viewed at wileyonlinelibrary.com]

detectors. Gating on AF-1 we identified a dominant population with the phenotype that defines stellate cells, the fibroblasts specific to the liver. This population has previously been reported to be endowed with AF in a limited analysis using conventional FCM because stellate cells store vitamin A in cytoplasm granules [14]. The second AF signal, AF-2, was found in epithelial cells (expressing CD324) that, at E18.5, could be subdivided into two subsets. The first expressed CD326 which is specific, at this stage, of newly differentiated cholangiocytes [19], and the second expressed the highest levels of CD324 while lacking CD326 and was consequently classified as hepatoblasts-like cells because they resemble E14.5 hepatoblasts [16, 17].

Irrespective of the cell preparation method, enzymatic digestion or mechanical dissociation, the two autofluorescent signals were detected, although mechanical dissociation resulted in lower representation of stellate cells and hepatoblast-like cells. We conclude that the two independent AF signals in stromal FL populations were intrinsic properties of the cells which confers reliability to the analysis. The transcriptional profile of the AF populations unambiguously confirmed the lineage affiliation proposed by the surface marker analysis.

The AF-2 parameter allowed the distinction of hepatocytes from hepatoblast-like cells ($CD324^+$ $CD326^-$ cells), by clearly demarcating the limits between the two cell types. Because hepatoblast-like cells rapidly decrease after birth, as most proliferative activity in the adult liver is driven by hepatocytes, we analyzed liver cells after birth. We found that the two different AF signals persisted at these later time points with AF-2 marking a majority of hepatoblast-like cells. Interestingly, most cholangiocytes lost AF-2 at P3 and virtually all were $AF2^-$ at P9. AF-2 is therefore the only property specific for hepatoblast-like cells, after birth. Although hepatocytes are the most numerous cells in the adult liver, they comprised less than 20% of the cell suspension analyzed here. This observation is consistent with the well-documented fragility of hepatocytes. The protocols currently recommended to isolate viable hepatocytes include enzymatic digestion similar to the procedure used in this study [21]. Alternatively, a perfusion with an enzymatic solution is followed by a purification in a Percoll gradient [22]. In any of these methods, $5–20 \times 10^6$ hepatocytes [21] (1%–6%) can be obtained out of the 3×10^8 hepatocytes in a mouse liver [23] indicating that no efficient procedure is currently available to isolate hepatocytes.

Our study presents several innovations: (1) The ID7000 software analysis provides an easy tool to detect independent AF signals; (2) The unmixing algorithm subtracts the AF signals to allow accurate true fluorescence detection, a feature already present in the SP6800; (3) Importantly, the analytical tool treats the AF signals as fluorescence and increases, therefore, the panel of analyzed parameters. We provide evidence that these advances will be invaluable to the characterization of single-cell suspensions obtained from autofluorescent tissues, difficult to analyze in conventional FCM.

ACKNOWLEDGMENTS

We thank all members of the FCM core facility, the members of the Institut Pasteur laboratory, Antonio Bandeira, Paulo Vieira, Rachel Golub and Pablo Pereira. This work was financed by the Institut Pasteur, INSERM, ANR (grant Twothyme, grant DELSTAR and grant EPI-DEV), REVIVE Future Investment Program and Pasteur-Weizmann Foundation through grants to A.C. This work was financed by Portuguese funds through FCT/MCTES in the framework of the project PTDC/MED-OUT/32656/2017 (POCI-01-0145-FEDER-032656). F.S. S is funded by the REVIVE Future investments postdoctoral grant (Investissement d'Avenir; ANR-10-LABX-73). MP is funded by FCT grant SFRH/BD/143605/2019.

AUTHOR CONTRIBUTIONS

Marcia Peixoto: Conceptualization (equal); data curation (equal); formal analysis (equal); investigation (equal); methodology (equal); writing – original draft (equal); writing – review and editing (equal). **Francisca Soares da Silva:** Conceptualization (equal); data curation (equal); formal analysis (equal); investigation (equal); methodology (equal); writing – original draft (equal); writing – review and editing (equal). **Sandrine Schmutz:** Data curation (equal); formal analysis (equal); methodology (equal). **Marie-Pierre Mailhe:** Data curation (equal); formal analysis (equal). **Sophie Novault:** Conceptualization (equal); data curation (equal); formal analysis (equal); investigation (equal); methodology (equal); project administration (equal); supervision (equal); writing – original draft (equal). **Ana Cumano:** Conceptualization (equal); data curation (equal); funding acquisition (equal); project administration (equal); supervision (equal). **Cedric Ait-Mansour:** Conceptualization (equal); data curation (equal); formal analysis (equal); investigation (equal); methodology (equal); project administration (equal); supervision (equal); validation (equal).

CONFLICT OF INTEREST

Cedric Ait-Mansour is working for the company Sony Europe B.v as a global senior manager market development-new products. All other authors declare no competing interests.

DATA AVAILABILITY STATEMENT

A version of this manuscript is available in BioRxiv bioRxiv 2021.09.29.462345; doi: https://doi.org/10.1101/2021.09.29.462345. FCM data has been deposited in Flow Repository under the name "FL autofluorescence."

ORCID

Francisca Soares-da-Silva https://orcid.org/0000-0003-1312-7601
Sophie Novault https://orcid.org/0000-0001-5708-3597
Ana Cumano https://orcid.org/0000-0002-4578-959X

REFERENCES

1. Robinson JP. Spectral flow cytometry-quo vadimus. Cytometry A. 2019;95:823.
2. Spitzer MH, Nolan GP. Mass cytometry: single cells. Many Features Cell. 2016;165:780–91.
3. Basiji DA. Principles of Amnis imaging flow cytometry. Methods Mol Biol. 2016;1389:13.
4. Stoeckius M, Hafemeister C, Stephenson W, Houck-Loomis B, Chattopadhyay PK, Swerdlow H, et al. Simultaneous epitope and transcriptome measurement in single cells. Nat Methods. 2017;14:865–8.
5. Nolan JP, Condello D. Spectral flow cytometry. Curr Protoc Cytom. 2013;63:1–13.

6. Cossarizza A, Chang HD, Radbruch A, Acs A, Adam D, Adam-Klages S, et al. Guidelines for the use of flow cytometry and cell sorting in immunological studies (second edition). Eur J Immunol. 2019;49:1457–973.
7. Grégori G, Patsekin V, Rajwa B, Jones J, Ragheb K, Holdman C, et al. Hyperspectral cytometry at the single-cell level using a 32-channel photodetector. Cytometry A. 2012;81:35–44.
8. Futamura K, Sekino M, Hata A, Ikebuchi R, Nakanishi Y, Egawa G, et al. Novel full-spectral flow cytometry with multiple spectrally-adjacent fluorescent proteins and fluorochromes and visualization of in vivo cellular movement. Cytometry A. 2015;87:830–42.
9. Schmutz S, Valente M, Cumano A, Novault S. Spectral cytometry has unique properties allowing multicolor analysis of cell suspensions isolated from solid tissues. PLoS One. 2016;11:e0159961.
10. Schmutz S, Valente M, Cumano A, Novault S. Analysis of cell suspensions isolated from solid tissues by spectral flow cytometry. J Vis Exp. 2017;123:55578.
11. Valente M, Resende TP, Nascimento DS, Burlen-Defranoux O, Soares-da-Silva F, Dupont B, et al. Mouse HSA+ immature cardiomyocytes persist in the adult heart and expand after ischemic injury. PLoS Biol. 2019;17:e3000335.
12. Pinho S, Frenette PS. Haematopoietic stem cell activity and interactions with the niche. Nat Rev Mol Cell Biol. 2019;20:303–20.
13. Soares-da-Silva F, Peixoto M, Cumano A, Pinto-do-Ó P. Crosstalk between the hepatic and hematopoietic systems during embryonic development. Front Cell Dev Biol. 2020;8:612.
14. Kubota H, Yao HL, Reid LM. Identification and characterization of vitamin A-storing cells in fetal liver: implications for functional importance of hepatic stellate cells in liver development and hematopoiesis. Stem Cells. 2007;25:2339–49.
15. Soares-da-Silva F, Freyer L, Elsaid R, Burlen-Defranoux O, Iturri L, Sismeiro O, et al. Yolk sac, but not hematopoietic stem cell-derived progenitors, sustain erythropoiesis throughout murine embryonic life. J Exp Med. 2021;218(4):e20201729.
16. Yang L, Wang WH, Qiu WL, Guo Z, Bi E, Xu CR. A single-cell transcriptomic analysis reveals precise pathways and regulatory mechanisms underlying hepatoblast differentiation. Hepatology. 2017;66:1387–401.
17. Nierhoff D, Levoci L, Schulte S, Goeser T, Rogler LE, Shafritz DA. New cell surface markers for murine fetal hepatic stem cells identified through high density complementary DNA microarrays. Hepatology. 2007;46:535–47.
18. Si-Tayeb K, Lemaigre FP, Duncan SA. Organogenesis and development of the liver. Dev Cell. 2010;18:175–89.
19. Tanaka M, Okabe M, Suzuki K, Kamiya Y, Tsukahara Y, Saito S, et al. Mouse hepatoblasts at distinct developmental stages are characterized by expression of EpCAM and DLK1: drastic change of EpCAM expression during liver development. Mech Dev. 2009;126:665–76.
20. Tan KS, Kulkeaw K, Nakanishi Y, Sugiyama D. Expression of cytokine and extracellular matrix mRNAs in fetal hepatic stellate cells. Genes Cells. 2017;22:836–44.
21. Jung Y, Zhao M, Svensson KJ. Isolation, culture, and functional analysis of hepatocytes from mice with fatty liver disease. STAR Protoc. 2020;1:100222.
22. Fry JR, Jones CA, Wiebkin P, Bellemann P, Bridges JW. The enzymic isolation of adult rat hepatocytes in a functional and viable state. Anal Biochem. 1976;71:341–50.
23. Falconer DS, Gauld IK, Roberts RC. Cell numbers and cell sizes in organs of mice selected for large and small body size. Genet Res. 1978;31:287–301.

SUPPORTING INFORMATION

Additional supporting information may be found in the online version of the article at the publisher's website.

How to cite this article: Peixoto MM, Soares-da-Silva F, Schmutz S, Mailhe M-P, Novault S, Cumano A, et al. Identification of fetal liver stroma in spectral cytometry using the parameter autofluorescence. Cytometry. 2022;101(11):960–9. https://doi.org/10.1002/cyto.a.24567